Theoretical Study of Model Tryptophan Radicals and Radical Cations: Comparison with Experimental Data of DNA Photolyase, Cytochrome *c* Peroxidase, and Ribonucleotide Reductase

Fahmi Himo and Leif A. Eriksson*

Department of Physics, Stockholm University, Box 6730, S-113 85 Stockholm, Sweden

Received: March 24, 1997; In Final Form: June 2, 1997[⊗]

Model systems of the tryptophan radical, present in several biological systems such as DNA photolyase, cytochrome *c* peroxidase, and mutated ribonucleotide reductase, have been investigated using gradient-corrected density functional theory (DFT). We report calculated spin densities and complete hyperfine tensors for all atoms, as well as potential energy and β-proton hyperfine tensor curves for the rotation about the C3−Cβ bond. Effects of hydrogen bonding to the N1 nitrogen (neutral radical) or N1−H hydrogen (cationic radical) are investigated, as is the C3 dioxygen adduct (peroxide) radical. Throughout comparisons are made to experimental data and previous theoretical studies of tryptophan model systems. The calculations support the earlier assignments of neutral Trp radicals present in mutant Y122F *Escherichia coli* ribonucleotide reductase at low temperatures, but most likely charged radical cations in DNA photolyase and yeast cytochrome *c* peroxidase. Although the calculations give clear-cut answers to, for example, the geometric arrangements, they are unable to resolve all of the ambiguities regarding the Trp radicals in the above systems, primarily due to lack of sufficient well-resolved data to compare with.

1. Introduction

In recent years, the discovery of amino acids as stable or transient intermediates in electron/hydrogen transport mechanisms in biological systems has gained significant attention. The most well-characterized systems are the tyrosine radicals in photosystem II and in ribonucleotide reductases (RNR). The larger tryptophan radical is also believed to have been observed in at least three different systems: cytochrome *c* peroxidase (CcP),[1−4] Y122F mutant *Escherichia coli* RNR,[5,6] and DNA photolyase.[7−10] One of the main problems hitherto addressed in the experimental work on tryptophan radicals has been to determine whether they are neutral or cationic, i.e., if the N1 nitrogen has lost its proton or not.

In DNA photolyase, Kim et al.[10] showed, by comparing experimental spin densities to results from semiempirical INDO and Hückel calculations, that the photoreduction of the flavinoradical $FADH^0$, caused by the tryptophan residue Trp306, is achieved by electron-transfer and not H-transfer; i.e., the tryptophan radical is cationic.

In CcP it was shown utilizing different experimental and theoretical methods that the radical present in the two-electron-oxidized intermediate, *compound ES*, is the cation of the tryptophan residue Trp191. This is furthermore weakly spin-coupled via a sequence of hydrogen bonds to the residues Asp235 and His175, to the $S = 1$ $(Fe{=}O)^{2+}$ heme group.[4]

The tryptophan radicals in the RNR subunit R2 were obtained from mutation, whereby the tyrosyl radical (Y122) present in the wild-type proteins was replaced by an "inert" phenylalanin (F). Thereby the di-iron center of the protein is forced to fetch its reducing equivalences from elsewhere, the nearby tryptophan residues Trp48, Trp107, and Trp111 being strong candidates. By comparing with computed hyperfine data and spin densities from density functional theory (DFT) calculations, it was concluded[6] that the tryptophan radicals—like the tyrosyl radical present in the wild-type protein—in this case are neutral and that the radical species observed at 20 K is different from that found at 77 K and room temperature. On the basis of ESR and ENDOR data combined with semiempirically derived β-proton hyperfine couplings, using X-ray crystallography geometric data[11] for the three Trp residues, W111 was found to be the radical observed at 20 K, whereas at higher temperatures the radical is shifted to the nearby residue W107. The apparent temperature-dependent H-transfer from W107 to W111 in the interval $T = 20-77$ K was, however, not addressed.

Other systems involving tryptophan residues interacting with a radical site is the tyrosyl radical in galactose oxidase, where a tryptophan is known to form a sandwich complex with the tyrosyl radical ring system,[12] the covalently bonded tryptophan tryptophyl−semiquinone cofactor radical in methylamine dehydrogenase of *Paracoccus denitrificans*,[13] and the peroxidation product in the oxidation cycle of Metmyoglobin (metMb) whereby a tryptophan−peroxide radical is believed to be formed.[14]

Several theoretical studies of tryptophan or the model system indole radical or radical cation have been reported.[1,6,15−19] Semiempirical Hückel−McLachlan calculations on the neutral and cationic indole radicals by Hoffman et al.[1] revealed significant differences in π-spin density on the nitrogen (0.30 vs 0.04 e^-) and the neighboring C2 carbon (0.04 vs 0.42 e^-) on the neutral and cationic systems, respectively. On C3 (connecting the indole side group to the protein backbone) both models displayed large spin densities (0.39 e^-). The corresponding data for the CcP compound ES radical, as derived from experiment by Huyett et al.[4] is 0.14 e^- on N1, 0.35 e^- on C2, and 0.41 e^- on C3.

Krauss and Garmer reported on restricted open shell Hartree−Fock (ROHF) and first-order configuration interaction (FOCI) calculations on indole, its neutral radical, and the radical cation, including solvent effects.[18] The reported ROHF data clearly give erroneous π-spin densities, due to the lack of spin polarization effects. However, their FOCI computed excitation energies and proton affinities indicated that the radical actually observed in CcP is the neutral radical and not the radical cation of Trp191. This level of computation was later questioned by

[⊗] Abstract published in *Advance ACS Abstracts,* November 1, 1997.

S1089-5647(97)01041-9 CCC: $14.00 © 1997 American Chemical Society

SCHEME 1

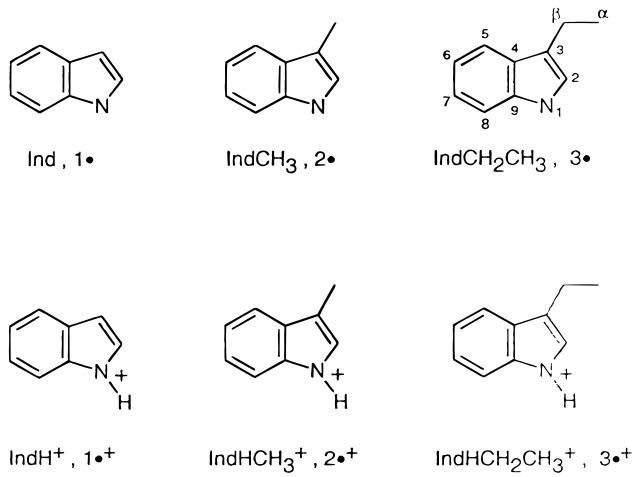

Serrano-Andrés and Roos[20] who determined more accurate excitation energies in the indole molecule, also including the effects of polar and nonpolar solvents, using complete active space SCF (CASSCF).

Jensen and co-workers[15] employed second-order perturbation theory (MP2) and hybrid Hartree−Fock density functional theory (HF-DFT) methods (the B3LYP functional) to investigate 3-methylindole and its neutral and cationic radicals. Their computed B3LYP/TZ2P spin densities on N1, C2, and C3 are (0.31, −0.13, 0.60) for the neutral system and (0.14, 0.19, 0.37) for the cation, which hence supports the original conclusion that the CcP tryptophan radical is in fact cationic. It was furthermore concluded that the DFT data was far superior to the MP2 results.

The same year, Walden and Wheeler published two studies utilizing density functional methods at the local, gradient-corrected and hybrid levels to investigate the indolyl radical and radical cation.[16,17] Their computed spin densities, using a lower level basis set (6-31G(d)), are slightly smaller than those reported by Jensen et al. but display the same general features. They also reported on isotropic hyperfine couplings obtained at the SVWN/6-31G(d), BLYP/6-31G(d), B3LYP/6-31G(d), and B3LYP/6-311G(d,p) levels, although the main emphasis was on a determination of the vibrational spectra of the systems. O'Malley and Ellson have also reported on the full hyperfine tensors for the neutral and cationic radicals of 3-methylindole, computed at the B3LYP/EPR−III level of theory.[19]

In the joint experimental and theoretical paper on RNR,[6] finally, Lendzian et al. reported spin densities from DFT calculations at the BPW/DNP level. These were used in order to derive complete hyperfine tensors that could assist in determining the nature and location of the observed (neutral) tryptophan radicals in Y122F mutant *E. coli* RNR.

In the present work, we have used gradient-corrected DFT at the PWP86/IGLO-III level, previously shown to yield highly accurate hyperfine data,[21−27] to calculate the complete hyperfine tensors of the neutral and cationic radicals of indole (**1**•, **1**•+), 3-methylindole (**2**•, **2**•+), and 3-ethylindole (**3**•, **3**•+) (Scheme 1). In particular, the effects of rotation about the C3−Cβ bond on the β-proton hyperfine couplings are investigated, as a means to determine the local orientation of the experimentally observed tryptophan radicals. We have also included effects of hydrogen bonding, believed to be present in several of the experimentally reported systems, as well as a study of the O_2-tryptophan peroxide adduct. These aspects, critical for the stability and functionality of the radicals in question, have not been addressed in detail in previous theoretical work.

2. Computational Details

All geometries, energies, and hyperfine parameters are computed using gradient-corrected density functional theory (DFT), as implemented in the linear combination of Gaussian type orbtials density functional theory (LCGTO-DFT) program deMon.[28] The gradient corrections are those by Perdew[29] for the correlation potential and by Perdew and Wang[30] for the exchange terms.

The orbital basis sets used for the hyperfine structure calculations are of IGLO-III type,[31] which are based on Huzinaga's 11s7p series,[32] very loosely contracted, and to which a double set of polarization functions is added. To speed up the calculations, the geometries were optimized throughout using the smaller local density optimized double-ζ plus valence polarization (DZVP) bases by Andzelm et al.,[33] followed by single-point DFT-ESR calculations with the larger IGLO basis sets. Initial tests showed that the DZVP basis yielded slightly longer bonds than IGLO-III but that the spin densities and hyperfine properties were essentially unaffected by the small geometrical differences.

For all the systems investigated, the spin contamination is found to be very low; the value of $\langle S^2 \rangle$ is less than 0.760. No vibrational frequencies or zero-point energies (ZPE) are included in the study.

The hyperfine coupling constants are results of the interaction between the unpaired electrons and the various magnetic nuclei. The full 3×3 hyperfine interaction tensor can be separated into two parts: the isotropic (spherically symmetric) component and the remaining anisotropic (dipolar) part. The isotropic component is related to the diagonalized full hfcc tensor via its trace: $A_{\mathrm{iso}} = {}^1/_3\ \mathrm{Tr}\{\mathbf{A}\}$. From a computational point of view, it can easily be calculated from the equation

$$A_{\mathrm{iso,N}} = \frac{4\pi}{3} g\beta g_{\mathrm{N}}\beta_{\mathrm{N}} \langle S_z \rangle^{-1} \sum_{\mu,\nu} P_{\mu,\nu}^{\alpha-\beta} \langle \phi_\mu | \delta(\mathbf{r}_{k\mathrm{N}}) | \phi_\nu \rangle$$

In this expression, $P_{\mu,\nu}^{\alpha-\beta}$ is an element of the spin density matrix, g and β are the electronic g-factor (taken as free electron value, 2.0023) and Bohr magneton, respectively, g_{N} and β_{N} are the corresponding nuclear terms, and $\langle S_z \rangle$ is the value of the spin angular momentum ($^1/_2$ for doublet systems).

3. Geometries and Spin Density Distributions

In Table 1 we list the PWP86/DZVP optimized geometrical parameters for the neutral and charged ethylindole radicals investigated in the present work. A comparison with the geometries obtained at the B3LYP and BLYP/6-31G(d) levels on the smaller neutral and charged indoles (**1**• and **1**•+),[16,17] and the B3LYP data on 3-methylindole (**2**• and **2**•+)[15] shows a very close similarity in the PWP86 and BLYP optimized geometries (differences well within 0.005 Å), similarly to earlier findings for the tyrosyl radical and radical cation.[21,36] The B3LYP geometries, on the other hand, display a slightly more compressed overall geometric structure. The largest modifications to the geometry (although still small) come from adding a methyl group to the 3-position; extending this by one more carbon has very little effect on the geometries. Observe that the numbering order of the atoms in tryptophan ring system varies between authors—the labeling used in the present work is displayed in Scheme 1, and all previous data discussed has been "converted" into the present numbering scheme.

The optimized dihedral angles θ(C2−C3−Cβ−Cα) in the ethyl-substituted systems are 92.3° (neutral) and 89.0° (cation), respectively. We also optimized the systems with the α-carbon

TABLE 1: PWP86/DZVP Optimized Geometric Parameters (Å/deg) for the Ethylindole Radical and Radical Cation Displayed in Scheme 1

	$indCH_2CH_3$	$indHCH_2CH_3^+$
	Distances	
N1−H1		1.022
N1−C2	1.339	1.352
C2−C3	1.453	1.441
C3−Cβ	1.504	1.498
Cβ−Cα	1.555	1.561
C3−C4	1.440	1.435
C4−C9	1.439	1.431
C4−C5	1.409	1.420
C5−C6	1.415	1.412
C6−C7	1.409	1.407
C7−C8	1.425	1.430
C8−C9	1.393	1.390
C9−N1	1.427	1.418
	Angles	
C9−N1−C2	104.6	109.9
N1−C2−C3	114.1	109.6
C2−C3−Cβ	127.8	125.3
C3−Cβ−Cα	112.6	112.3
C2−C3−C4	104.5	105.8
C3−C4−C9	105.5	107.9
C4−C9−N1	111.3	106.8
C9−C4−C5	120.7	119.1
C4−C5−C6	118.4	118.7
C5−C6−C7	120.5	120.8
C6−C7−C8	121.5	121.6
C7−C8−C9	118.1	116.8
C8−C9−C4	120.7	123.0
	Dihedrals	
C2−C3−Cβ−Cα	92.3	89.0

TABLE 2: PWP86/IGLO−III Computed Spin Densities for the Different Tryptophan Radical Models of Scheme 1

atom	ind	$indCH_3$	$indCH_2CH_3$	$indH^+$	$indHCH_3^+$	$indHCH_2CH_3^+$
N1	0.250	0.267	0.261	0.119	0.142	0.143
C2	−0.074	−0.081	−0.076	0.144	0.167	0.166
C3	0.553	0.549	0.556	0.334	0.355	0.361
C4	−0.109	−0.101	−0.105	−0.069	−0.086	−0.085
C5	0.224	0.191	0.194	0.286	0.246	0.243
C6	−0.051	−0.037	−0.040	−0.076	−0.058	−0.057
C7	0.175	0.145	0.151	0.194	0.156	0.152
C8	0.031	0.024	0.021	0.115	0.089	0.092
C9	0.068	0.063	0.063	0.030	0.027	0.022
Cβ		−0.046	−0.048		−0.023	−0.028
Cα			0.034			0.035

lying in the plane of the ring system, at $\theta = 0$ and 180°. These points were found to lie 1.20 and 1.65 kcal/mol above the ground state for the neutral system and 0.25 and 1.15 kcal/mol above the optimized ground state for the cation, respectively. The potential surface for rotation about the C3−Cβ bond is hence—as in the case for tyrosine radicals[21]—very flat. This indicates that the systems will have a large flexibility and will be able respond geometrically to optimize hydrogen bonding and other interactions from neighboring groups.

The PWP86/IGLO-III//DZVP unpaired spin densities on the heavy atoms, obtained from Mulliken population analyses, are reported in Table 2 for the six systems studied in the present work. The absolute spin densities are less than 0.04 for all hydrogens and thus not included in the table. Again, there is a very close agreement (within 0.02) between the present indole or 3-methylindole data and those obtained at the BLYP/6-31G-(d) level.[17] The B3LYP approach, on the other hand, tends to give numerically larger spin densities,[15,17] and thus also larger differences between the positive and negative contributions than do the pure DFT methods BLYP and PWP86, irrespective of basis set used. The differences in spin density distributions between the neutral and the cationic radicals are clearly displayed. In the work by O'Malley and Ellson,[19] only graphical representations of the unpaired spin densities were given (i.e., no numerical values). The overall pictures do, however, agree with the other DFT data discussed here.

TABLE 3: ^1H, ^{13}C, and ^{14}N Isotropic Hyperfine Coupling Constants in G, Computed at the PWP86/IGLO−III//DZVP Level

	A_{iso}					
atom	ind	$indCH_3$	$indCH_2CH_3$	$indH^+$	$indHCH_3^+$	$indHCH_2CH_3^+$
N1	2.3	2.6	2.5	1.2	1.3	1.4
C2	−7.3	−7.3	−7.2	0.4	0.8	0.6
C3	16.5	15.9	15.8	8.1	8.5	8.3
C4	−8.7	−7.9	−8.0	−6.7	−6.6	−6.6
C5	6.6	4.9	5.3	8.4	6.9	6.6
C6	−4.3	−3.5	−3.6	−5.5	−4.4	−4.2
C7	4.2	3.3	3.6	5.1	3.8	3.6
C8	−1.0	−1.0	−1.2	1.4	0.9	1.0
C9	0.3	0.1	0.2	−1.1	−0.9	−1.1
Cβ		−6.3	−5.9		−4.1	−3.7
Cα			13.5			7.7
H1				−2.9	−3.5	−3.4
H2	−0.2	−0.4	−0.5	−3.9	−4.8	−4.7
H3	−11.6			−7.6		
H5	−4.7	−4.0	−4.0	−6.0	−5.1	−5.1
H6	0.5	0.2	0.3	0.9	0.6	0.6
H7	−3.7	−3.1	−3.2	−4.5	−3.6	−3.5
H8	−0.1	−0.8	−0.8	−2.4	−2.1	−2.1
Hβ1		1.2	2.9		6.2	3.3
Hβ2		17.4	10.8		6.1	8.4
Hβ3		26.4			26.6	
Hα1			2.5			2.6
Hα2			−1.0			−0.4
Hα3			−0.9			−1.0

In contrast to the geometries, the alkyl substituents do have an effect on the spin densities on both nitrogen and the carbons. This results, for example, in a better agreement for the ethyl-substituted species with both the CcP compound ES[4] (cation) and the mutant RNR tryptophan radical[6] (neutral), than what is observed for the corresponding indole or 3-methylindole systems. The agreement between experiment and theory is for almost all atoms within 0.05; the main exception is the C2 spin density in CcP, where Huyett et al. derived the value 0.35, a value that no theoretical method thus far has been close to. A possible explanation for this deviation could be the use of an erroneous *Q*-value in the experimental conversion from isotropic proton hyperfine coupling on H2 to spin density on C2. The very large shifts in spin densities on N1 and C2 but essentially constant value on C3 when comparing the neutral and cationic species, as predicted by semiempirical Hückel−McLachlan and INDO calculations,[1,10] are clearly not correct.

4. Hyperfine Properties

Previously, O'Malley and Ellson have published B3LYP/EPR-III computed hyperfine tensors of neutral 3-methylindole radical and radical cation.[19] In Table 3, we list the computed PWP86/IGLO-III isotropic components for all six systems investigated in the present work, and in Table 4 we show the components of the diagonalized full hyperfine tensors **A** for all nuclei in the 3-ethylindole radical and radical cation. In Table 5 we list the available experimental data for the different tryptophan radicals encountered in proteins.

The odd-alternant character of the spin distribution is also reflected in the isotropic hyperfine couplings. Comparing with the previously reported isotropic couplings of **1**$^\bullet$ and **1**$^{\bullet+}$ obtained at various DFT levels by Walden and Wheeler,[17] the present results are generally in nice agreement for the hydrogens (at most ±1.0 G deviation). For the heavy atoms the deviations

TABLE 4: Full Hyperfine Tensors for the 3-Ethylindole Systems (in G), Computed at the PWP86/IGLO-III//DZVP Level

	$indCH_2CH_3$			$indHCH_2CH_3^+$		
atom	A_{xx}	A_{yy}	A_{zz}	A_{xx}	A_{yy}	A_{zz}
N1	−1.7	−1.7	10.9	−1.3	−1.2	6.7
C2	−8.5	−6.9	−6.3	−5.4	−4.8	12.1
C3	0.8	1.1	45.5	−1.8	−1.2	27.9
C4	−11.1	−7.1	−5.8	−9.3	−5.8	−4.6
C5	0.3	0.4	15.2	0.1	0.2	19.5
C6	−4.6	−3.2	−2.9	−6.1	−3.4	−3.1
C7	−0.6	−0.3	11.7	−0.7	−0.5	12.1
C8	−2.5	−2.0	0.9	−2.0	−1.8	6.8
C9	−1.7	−1.0	3.3	−1.9	−1.0	−0.3
Cβ	−6.4	−5.8	−5.4	−4.5	−3.4	−2.6
Cα	12.3	12.4	15.8	6.4	6.4	10.3
H1				−6.7	−4.4	0.7
H2	−1.7	−1.0	1.2	−7.8	−5.7	−0.7
H5	−6.0	−4.5	−1.5	−7.9	−5.6	−1.8
H6	−0.3	0.1	1.1	−0.1	0.5	1.4
H7	−5.5	−3.5	−0.8	−5.8	−3.1	−0.8
H8	−1.5	−1.0	0.1	−3.3	−2.8	−0.2
Hβ1	2.0	2.0	4.7	2.3	2.8	4.8
Hβ2	9.7	10.1	12.5	7.4	8.0	9.7
Hα1	1.8	2.1	3.6	1.9	2.3	3.7
Hα2	−2.0	−1.2	0.2	−1.4	−0.3	0.5
Hα3	−2.0	−1.3	0.6	−2.0	−1.2	0.2

are somewhat larger. The PWP86 results appear to fall roughly halfway between the BLYP/6-31G(d) and the B3LYP/6-311G-(d,p) data of Walden and Wheeler. Comparing with the B3LYP/EPR-III results by O'Malley and Ellson, the data agrees to within ±1 G for essentially all couplings. The main differences occur for the isotropic N1, H2 (neutral), and H1 (cation) couplings, and the C2 tensor of the neutral system. For H5 (neutral), the tensor given by O'Malley and Ellson is apparently erratic. Throughout, the B3LYP results are numerically larger than the PWP86 data. This difference between the B3LYP and PWP86 approaches has previously been explored in detail,[35] and the tendency of the B3LYP functional to overestimate isotropic hfcc's of π-radicals was clearly demonstrated. As for the spin densities, the largest changes in isotropic hfcc's occur upon methyl substitution, rather than extending the methyl group to ethyl. The proton couplings are modifed up to 1 G in going from indole to 3-methylindole; for the heavy atoms the modifications are 1−1.5 G. The atoms displaying the largest differences between the neutral and corresponding cationic case are N1, C2, C3, and the ethyl tail. For the hydrogens, the cations overall display numerically larger couplings, with the biggest changes observed for H2.

The values for the β-protons of 3-ethylindole listed in Tables 3 and 4 are for the optimized geometries (ethyl tail approximately perpendicular to the plane of the ring). The values of A_{iso} (H_β) will vary considerably with rotational angle due to the modified interaction with the SOMO π-orbital of the ring system. In Figures 1 and 2 we show the variations in potential energy (A) and β-proton hyperfine tensors (B) as functions of rotational angle, for the neutral system (Figure 1) and the cation (Figure 2). The study was conducted such that the geometries were fully optimized at C2−C3−Cβ−Cα dihedral angles θ equal to 0, 90, and 180°. The geometric parameters for all atoms were then varied linearly between these optimized geometries for each rotational angle θ indicated in the figures, and restricted optimizations (to adjust the rotation of the terminal methyl group hydrogens) were performed at the PWP86/IGLO-III level. The

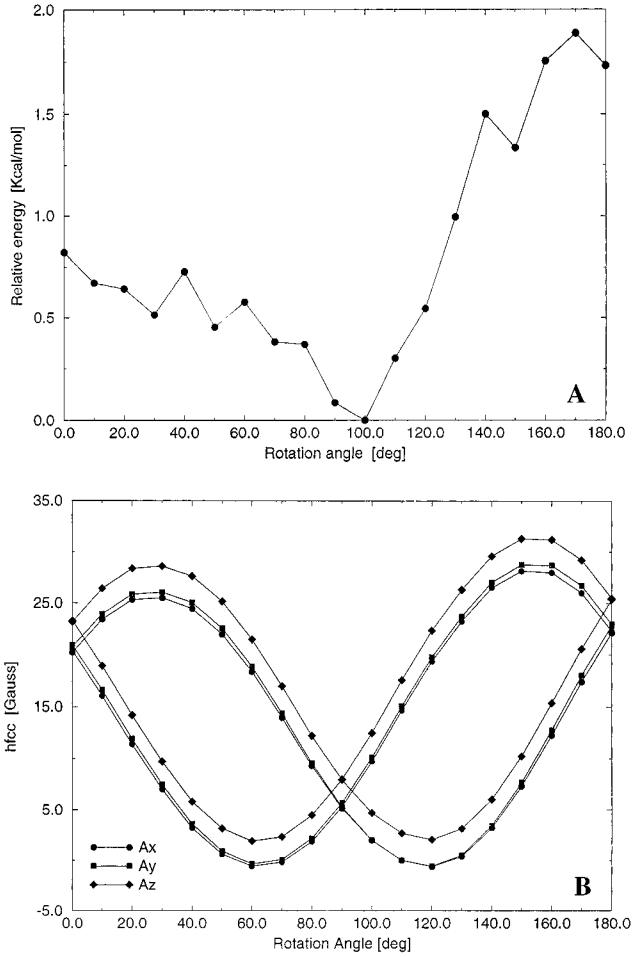

Figure 1. Rotational energy surface (A) and β-proton hyperfine tensor variations (B) for the neutral 3-ethylindole radical as functions of the C2−C3−Cβ−Cα rotational angle.

TABLE 5: Experimentally Assigned Tryptophan Radical Hyperfine Components, Detected in DNA Photolyase,[7−10] Cytochrome *c* Peroxidase,[1−4] and Ribonucleodtide Reductase[5,6] [a]

	DNA photolyase			CcP			RNR (W_a/W_b)		
atom	A_{xx}	A_{yy}	A_{zz}	A_{xx}	A_{yy}	A_{zz}	A_{xx}	A_{yy}	A_{zz}
^{14}N						0.2	(1)/2.2	(1)/2.2	10.5/8.7
^{15}N						0.3			
^{13}C2				−5.7	−5.7				
^{13}Cβ				−5	−5				
HN						5.9			
H2			5			5.3			
H5							−6.3/−7.0	−5.2/−6.5	(1.5)/−4.0
H6						1.8			
H7							−5.6/−6.0	−4.6/−3.8	(1.5)/−3.5
H(Hbond)							−1.2/-	1.9/-	−0.8/-
Hβ1			16			4.6	13.6/(2)	13.6/(2)	13.6/(2)
Hβ2			16			7.5	28.3/16.0	28.3/16.0	28.3/16.0

[a] All components listed are in G. Values in parentheses indicate estimated maximum absolute value of the coupling.

very restricted optimizations performed cause the "jagged" stuctures of the energy curves.

For both the neutral and the cationic systems, there is a clear global minimum at ca. 90−100° rotational angle. Rotational motion toward smaller values of θ (moving Cα away from the six-membered ring) is associated with a very small barrier, 0.6−0.8 kcal/mol, whereas the barrier is slightly larger for larger values of θ. The overall energetics involved are, however, less than 2 kcal/mol for both systems, analogous to our previous work on the tyrosyl radical.[21] The energy barrier to rotation is lower for the cation than for the neutral radical.

The hyperfine tensors of the β-protons show large, sinusodial variations (also here, in analogy to the tyrosyl radical). The curves for the two hydrogens cross at the rotational angles where they are symmetrically placed with respect to the ring plane, at $\theta = 0$, 90, and 180°. With the exception of two components at rotational angles close to 60 and 120°, all hyperfine tensor components are positive. Furthermore, the curves for the neutral (1B) and cationic (2B) systems are almost identical with slightly larger values for the neutral system. Comparing the data displayed in the two graphs to experimental data for the β-hydrogens, one can obtain important information about the relative orientation of the tryptophan radical in question.

The different empirical parameters (Q and B) generally employed to deduce carbon spin densities from the corresponding α- and β-proton hyperfine values can easily be derived using the computed data in Tables 2 and 3.

5. Comparison with Trp Radicals in Biological Systems

5.A. DNA Photolyase. In DNA photolyase, two different proton couplings have been observed: a stable triplet (2 H) with a splitting of 16−17 G and a transient doublet (1 H) with a splitting of ca. 5 G.[9,10] Comparing with the full hf tensors in Table 4, we can tentatively assign the transient 5 G splitting as arising from either of H5 or H7 of the neutral system, or H2, H5, H7, or H_N of the cation. The 5 G doublet was found to vanish in the deuterated species Trp-d_5 and Trp-2,6-d_2 (our labeling), which thus is consistent with the cation H2 position only. Interesting to note is that the Hückel−McLachlan data for the ring protons,[1] although supporting the assignment as the 5 G splitting arising from H2 of the cation, deviate considerably for the remaining hyperfine tensor components from those obtained at the DFT level.

The smaller hyperfine tensor expected for nitrogen in the cation than in the neutral system was also taken as evidence for the cationic nature of the Trp306 radical. Although the main component for ^{14}N is indeed smaller (10.7 G in neutral 3-ethylindole vs 6.6 G in the cation), the differences are not huge. Again, the DFT computed hyperfine components differ considerably from the data obtained from the Hückel−McLachlan calculations (neutral: 3.0, 3.0, 18 G; cation: 0.4, 0.4, 2.4 G). The present results for 3-ethylindole are (−1.7, −1.7, 10.9) G and (−1.3, −1.2, 6.7) G, respectively, whereas O'Malley and Ellson predict the full tensors (−0.9, −0.8, 14.1) and (−0.8, −0.6, 7.9) G for the neutral and cationic 3-methylindole radicals, respectively.[19]

The 16 G triplet was in the experimental paper assigned to the two β-methylene protons. From Tables 4 and 5, we see that all hf tensor components of all the α-protons (neutral as well as charged species) are smaller than ±8 G and can thus not account for the observed 16 G splittings. For the β-protons, hyperfine couplings of 16 G are only found for one atom at a time (cf. Figures 1B and 2B), at rotational angles around 10, 70, 110, and 160°. The anisotropic couplings of the β-protons are small, ca. (−1, −1, +2) G, and do not vary upon rotation;

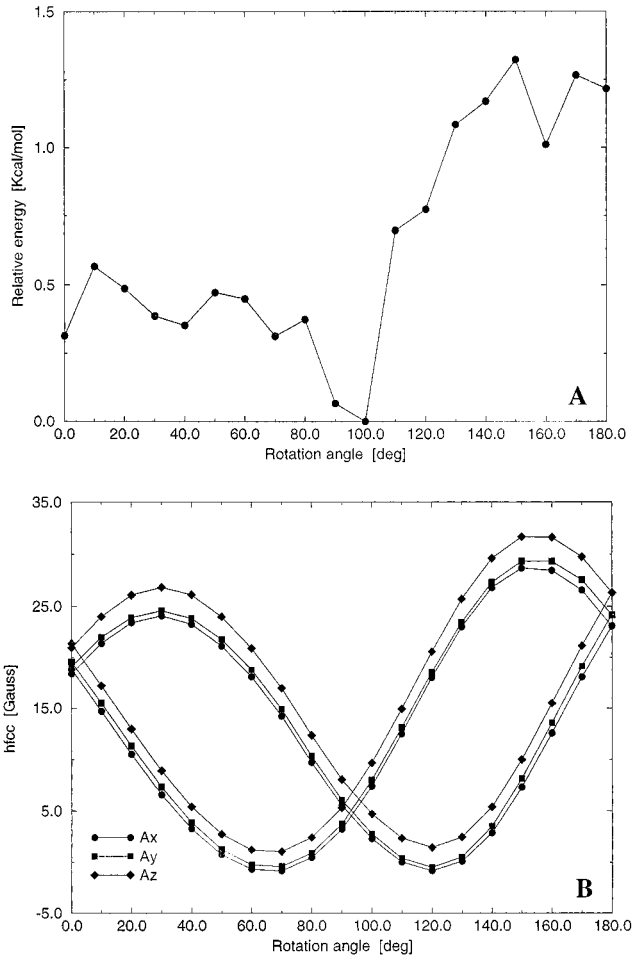

Figure 2. Rotational energy surface (A) and β-proton hyperfine tensor variations (B) for the 3-ethylindole radical cation as functions of the C2−C3−Cβ−Cα rotational angle.

instead all the modification to the hyperfine structure comes from the isotropic component. The present theoretical approach is known to yield ca. 80−85% of the experimental data, and it thus seems highly unlikely that in this isolated case we should be very far off. In the recent study on the tyrosyl radical, the β-methylene proton couplings were throughout in excellent accord with experimental data, for a large variety of RNR and PSII proteins. The possibilities for the observed 16 G triplet are thus that (a) the two couplings arise from very small values of the rotational angle—for the cation the main component is ca. 21 G at $\theta = 0$°, whereas for the neutral case it is 24 G—(b) that the protein is in an equilibrium geometry close to 90° and there undergoes rapid vibrational motion by ca. ±20° (energetically the vibrational energy of ca. 0.3 kcal/mol is sufficiently small), (c) the system observed in the experiments interacts very strongly with some neighboring group(s), or (d) the system observed in DNA photolyase is not Trp306. The results from theory and calculations deviate too much for a simple explanation of the hfcc of this particular system. If possible, experiments in which only the two β-protons of Trp306 are substituted for deuterons should be able to shed more light on this.

We finally also note that in the wild-type spectrum,[10] more fine structure is observed that disappears upon deuteration. These were, however, not analyzed in the original paper.

5.B. Cytochrome *c* Peroxidase. The second system where cationic Trp radicals are believed to be encountered is the CcP compound ES (Trp191). The most detailed experimental determination of the hyperfine parameters of this compound has been reported by Huyett et al.,[4] performing experiments on wild-

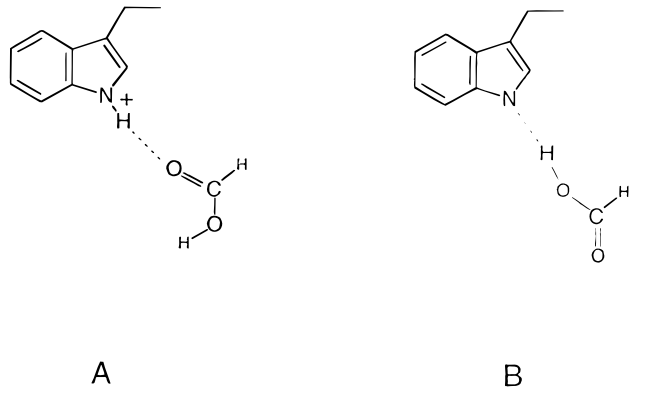

Figure 3. Models used to investigate the effects of hydrogen bonding to the tryptophan radicals. (A) 3-ethylindole radical cation H-bonding to formic acid (CcP model). (B) Neutral 3-ethylindole radical H-bonding to formic acid (RNR model). The $N-O_{Hbond}$ distances are 2.94 Å.

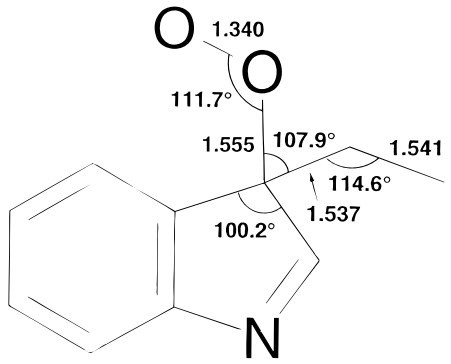

Figure 4. Optimized 3-peroxyl-3-ethylindole radical.

type and isotope-labeled systems at 2 K. In this protein, hydrogen bonding between Trp191 and a nearby aspartate group (Asp235) is known to be important. Calculations were hence performed both on the free cation and on the cation hydrogen bonding to a formic acid unit. The carbon atom of formic acid was placed at the position relative to the tryptophan as determined from X-ray crystallography,[37] whereafter partial optimization was performed on H_N and the remaining atoms (except carbon) in formic acid (Figure 4).

Huyett et al. report an exchangeable proton with $|A(H)|$ roughly 5.9 G and assign this, on the basis of results for selectively deuterated samples, to H_N in the cation. The computed value for the main component of H_N in 3-ethylindole radical cation is −6.7 G, in fair agreement with the experimental data. Modeling hydrogen bonding to the cation NH-group (Figure 3A) reduces the H_N main component to −6.5 MHz. However, also other couplings agrees with this (cf. Table 4), such as the main component on H7 and the middle component of H2 (cation), and the main components on H2, H5, and H7 in the neutral system. The ring protons are, however, in general not as easily exchangeable as the H_N proton in the cation will be, especially considering the presence of the H-bonding amino acid Asp235.

Keeping the sample in D_2O, or selectively exchanging the proton at C2 for deuterium, caused the intensity of the exchangeable proton in the ^1H spectra to be significantly reduced. This would speak in favor of the H2 middle component of the cation (−5.9 G) being responsible for the observed splitting; a possibility that is also discussed by Huyett et al. but discarded on the basis of the Hückel−MacLachlan spin densities. As seen from the above discussion, spin densities and hfcc's computed at the Hückel−MacLachlan level should, however, be viewed with a large degree of skepticism.

In the partially deuterated sample, two nonexchangeable couplings were observed in the ^2H spectra, corresponding to proton couplings of 5.3 and 1.8 G, respectively. These were assigned to the H2 and H6 positions, respectively. The latter agrees well with the main component on H6 (1.4 G) or the smallest component on H5 (−1.8 G) on the cation, although also that on H8 of the neutral species (ca −1.4 G) may explain the observed result. Hydrogen bonding does not affect the hfcc on the six-membered ring to any large degree. For the observed coupling of 5.3 G there are also several possibilities. The middle component of the H5 hyperfine tensor in the cation is −5.7 G; however, then the main component of −7.8 G should probably also be observable. Other candidates are, as mentioned above, the main components on H2, H_N or H7, in the presence of the hydrogen-bonding formic acid molecule. Worth noting is also the large amount of finer structure in the experimental spectrum—in the selectively deuterated (C2D,H) ^2H spectrum one could possibly identify couplings at 1 and 2 G (^1H scale), which would agree well with the couplings of H2 in the neutral systems. Hence, one possibility that should not be ruled out completely is that we actually have a mixture of the neutral and the cationic system—possibly caused by the H-bonding Asp235 group. The EPR spectra are recorded at $T = 2$ and 4 K; at higher temperatures the equilibrium may be shifted toward more of the neutral species, which would explain the absorption spectrum that has been assigned to a neutral species.[38] Temperature-dependent EPR spectra combined with dynamics studies of the Trp-H^+−Asp^- equilibrium might be able to shed further light on the problem of the CcP radical. Such dynamics are presently under investigation in our laboratory.

In the EPR experiments, two additional distinct ^1H proton couplings were clearly identified and found present also in the pentadeuterated sample: at 4.6 and 7.5 G. These were assigned to the β-protons. Using the conventional $\cos^2\theta$ relation between isotropic coupling constants and spin densities, the rotational angle for the β-protons were determined as −56 and +64°, respectively, defined from the plane perpendicular to the ring (a negative value corresponds to rotation toward the six-membered ring). This is in very close agreement with the X-ray crystallography data for Trp191 in wild-type CcP, −54.6° for the first proton (corresponding to θ (C2−C3−Cβ−Cα) = 95.4°).[37] In our Figures 1B and 2B, the hyperfine tensor components 7.5 and 4.6 G correspond to values of θ of 85 or 95° for the cation and ca. 80 or 100° for the neutral system; as seen, $\theta = 95°$ is in excellent agreement with the experimental data, also confirming the X-ray structure as representing the global minimum on the rotational potential curve.

From ^{13}C and ^{15}N isotope labeling specifically at C2, Cβ, and N1 positions, further information on the system was obtained. It was concluded that the perpendicular component to the π-orbital SOMO in C2, $A_\perp$ (^{13}C2), is ca. (−)5.7 G. The parallel component, which should be positive and twice as large, could not be detected experimentally. From our computed data listed in Table 4, we see that the perpendicular component of C2, obtained as $^1/_2(A_{xx} + A_{yy})$, is −5.1 G for the cation and −6.6 G for the neutral system. Hydrogen bonding to the cation (Figure 3A) or the neutral system (Figure 3B) modifies the carbon couplings slightly at the C2 position; now $A_\perp$ (^{13}C2) = −5.7 G for the cation and −6.0 G for the neutral radical. The corresponding data obtained by O'Malley and Ellson at the B3LYP/EPR-III level are −8.5 G for the neutral radical and −6.7 G for the radical cation of 3-methylindole.[19]

A slightly smaller coupling (5.3 G) was found in the experimental ENDOR spectrum of ^{13}Cβ. The PWP86/IGLO-III calculated values for Cβ are −5.7 G for the neutral system and −4.5 G for the cation (H-bond present). The corresponding

data obtained by O'Malley and Ellson for 3-methylindole is −6.4 and −4.1 G for the neutral and the cation, respectively.[19] From our calculations we note, however, a slight modification of the spin distribution and isotropic hfcc's of Cβ as a result of extending the alkyl tail from Me to Et (Tables 2 and 3).

For ^{14}N and ^{15}N, splittings of 0.6 and 0.8 MHz were reported. The calculated values, also for the smaller tensor components and in the presence of hydrogen bonding, all exceed this value by a factor of 3 at all levels hitherto employed. The smallest tensor is, however, found for the cation and may be taken as an indication of the cationic nature of the CcP Trp191 radical. The experimentally derived spin density on nitrogen is 0.14, which agrees excellently with our data for the cation, but not with the neutral system.

To sum up the findings for CcP and the correlation between theory and experiment for this system, we note that ambiguities do prevail regarding the identity and nature of the radical observed experimentally. These uncertainties are primarily related to the very low nitrogen couplings observed and, as for DNA photolyase, the fact that there are several proton hyperfine couplings that thus far have not been accounted for in the experimentally reported data sets. The best overall agreement is found when comparing results for the cationic species, although we do not rule out the possibility of a (temperature-dependent) equilibrium situation between the cation and the neutral radical, or between Trp and some other radical site. The initially suggested thioester bridge radical ($R-S-S-R^+$)[1] has not been investigated in the present work and has also been ruled out in later experimental work based on mutation experiments.

5.C. Ribonucleotide Reductase. In the ribonucleotide reductase R2 subunit, tryptophan radicals were observed upon mutation, whereby the naturally occurring tyrosyl radical site was removed/deactivated.[5,6] The ESR and ENDOR derived hf tensors led to the assignments listed in Table 5 and to the conclusion that the radicals observed here were neutral. Furthermore, it was seen that the radical site was shifted from Trp111 ("W_a") at low temperatures to Trp107 ("W_b") at 77 K and higher. The experimental assignments were supported by density functional and semiempirical calculations.

For the radical denoted W_a, the ^{14}N main component to the hyperfine tensor was determined to be 10.5 G, and the remaining ones were ca. 1 G each. As seen from Table 4, the large component agrees excellently with the computed data for the neutral system: 10.9 G (for the cation, 6.7 G). Using the hydrogen-bonding model with formic acid (Figure 3B), the main component is lowered to 10.1 G. The remaining components are slightly too large (−1.7 for the neutral, −1.3 for the cation), and negative. The experimentally derived isotropic component of 4.0 G was based on all components being positive ((10.5 + 1 + 1)/3). However, using the correct assignment we get $A_{iso}(N) = (10.5 - 1 - 1)/3 = 2.8$ G, in very close agreement with the presently computed value for the neutral 3-ethylindole radical: $A_{iso}(N) = 2.5$ G (2.4 G in presence of H-bond). The data reported by O'Malley and Ellson displays a much overestimated main component for the neutral system (14.1 G), whereas the small components are negative and just below 1 G in magnitude.

The β-proton couplings were determined from spectra to be fully isotropic, with components 13.6 and 28.3 G. This corresponds to a dihedral angle θ of 20 or 165° (Figure 1B). The corresponding dihedral angles for the hydrogens to the plane perpendicular to the rings are then (−10, −130) or (+5, +125)°, respectively. The X-ray structure for W111 gives the angles −10 and −132° for the two β-hydrogens,[11] in very nice agreement with the present results at $\theta = 20°$. In this case, like for the tyrosine radical in RNR, the amino acid is hence not in its relaxed ground-state geometry ($\theta \simeq 90°$), but in a position that lies energetically "uphill"—possibly at a local minimum—stabilized by hydrogen bonding, "steric" effects from neighboring amino acids, or similar conditions.

From deuterium-labeled samples, two α-proton tensors were observed as (−6.3, −5.2, ⩽ −1.5) and (−5.6, −4.6, ⩽ −1.5) G and assigned to positions H5 and H7. For the neutral system, this assignment seems entirely correct, although the computed couplings are on the low side. Also the H2, H5, H7, and H_N hydrogens of the cationic systems have similar hyperfine tensors, this time on the high side. As the present approach is known to yield on average ca. 85% of experimental isotropic ring proton couplings, the assignment to the neutral positions H5 and H7 seems very likely. The calculated values, without the hydrogen-bonding moiety, are (−6.0, −4.5, −1.6) and (−5.4, −3.5, −0.8) G, respectively. Including hydrogen bonding, these become slightly improved relative to experiment: (−6.2, −4.7, −1.6) and (−5.6, −3.6, −0.8) G. The corresponding isotropic couplings (exptl: −4.0 G; −3.6 G) agree well with the theoretically derived ones of −4.0 and −3.2 G. There is a very close agreement between our data set and that reported by O'Malley and Ellson.[19]

In the spectra of W_a-d_5 (Trp111), a small ^{1}H anisotropic tensor was also observed (−1.2, −0.8, 1.9 G), assigned to a proton forming a hydrogen bond to the nitrogen, at a distance of ca. 1.75 Å. This hydrogen bond will stem from the residue Glu204, whereas to Trp107, a water molecule is known to form hydrogen bonding.[11] In analogy with the tryptophan cation system, this effect was modeled using formic acid (Figure 3B), employing the same type of computational scheme. The hydrogen-bonding proton on the formic acid does indeed obtain a small anisotropic hf tensor, (−1.0, −0.9, 1.5) G, verifying the experimental findings beautifully. The isotropic component of this hydrogen is only −0.14 G and thus not detectable in the ESR experiment.

We now turn to the 77 K and room-temperature tryptophan radical W_b (Trp107). In the pentadeuterated sample, only one β-coupling (isotropic) could be observed, with the value 16.0 G. That the other proton could not be detected implies that it lies in the plane of the rings (the nodal plane of the π-symmetry SOMO). The values 16 vs 0 G correspond to a rotational angle θ of 65 or 115°. The rotational angles for the β-protons are then (−85, +155) or (+85, −155), respectively. The latter matches well the X-ray data for W107 (angles +87° and −153°). The result for the rotational analysis of the cationic radical is highly similar.

For the nitrogen atom, the isotropic coupling reported in ref 6 should again be reevaluated as $(8.7 - 2.2 - 2.2)/3 = 1.4$ G, as the hyperfine tensor components for both neutral and charged systems consist of one large positive and two small negative components. This yields an isotropic component on N1 that agrees excellently with that computed for the cation (Table 3), whereas the full hfcc tensor of the cation is smaller than that observed experimentally. These differences in the dipolar tensors for the nitrogen and the α-protons of W107 (cf. Tables 4 and 5) are not easily explained. On one hand, there will be larger vibrational motion at room temperature. Thereby averaging effects, which can influence both isotropic and anisotropic components, may be present. On the other hand, the observed nitrogen tensor appears to fall halfway between that of the neutral and the cationic case; for the increased H5 and H7 tensors, a better fit is at least in part obtained for the cation than for the neutral system (Table 4), cf. the above discussion on the neutral/charged equilibrium situation in CcP. The newly created radical center may also reorient to form a better

hydrogen bond to His241 or to interact more strongly with the di-iron center. It is clear, though, that the static X-ray geometry of a neutral radical at W107 does not fully explain the observed hyperfine structure at room temperature.

5.D. Peroxide Adduct. Using spin-trapping techniques, it has recently been shown[14] that a tryptophan radical is created during the oxidizing cycle of metmyoglobin. This tryptophan radical reacts rapidly with dioxygen to form a peroxide radical, as seen from the consumption of O_2 during the reaction and the simultaneous disappearance of the tryptophan EPR spectrum. In the spin-trapping experiments, 3,5-dibromo-4-nitrosobenzenesulfonic acid (DBNBS) was used to label tryptophan through the formation of a nitroso radical as DBNBS bonded covalently to the C3 position on tryptophan.

To investigate the spin properties of the tryptophan−peroxide complex, we let ground-state O_2 react with a neutral tryptophan radical at the C3 position. The optimized structure is schematically displayed in Figure 4. Upon peroxidation, the radical character is moved almost completely to the peroxide unit. The unpaired spin density is 0.34 on the inner oxygen and 0.65 on the outer, in excellent agreement with previous experimental and theoretical findings for various alkyl peroxide radicals.[39,40]

There is some isotropic hyperfine structure on the C3 carbon (A_{iso}(C3) = −4.0 G), which agrees well with both experimental[41] (−3.9 G) and theoretical[40] (−3.84 G) data on *tert*-butyl peroxide, $(CH_3)_3$ COO. The oxygen isotropic couplings, −8.4 G (inner) and −12.8 G (outer), are smaller than experimental data for the corresponding alkyl peroxide radical hfcc's (on average −13 and −23 G) but similar to the theoretical results obtained at the B3LYP level of theory.[40]

The largest theoretical isotropic component on the hydrogens is 1.1 G (H5). The anisotropic couplings are for all tryptophan atoms less than 1 G, with the one exception of H5 (main component 1.9 G). For the oxygens, the anisotropic data is highly similar to other peroxides: (−44, 21, 24) G for the inner and (−73, 36, 37) G for the outer oxygen.

This very brief study shows that the tryptophan peroxide radical, when formed, will display the same hyperfine structure as other peroxide radicals and will lose all its radical character on the tryptophan residue. This agrees very well with the findings from the spin-trapping experiments on metmyoglobin.

6. Conclusions

We have in the present work investigated several aspects of tryptophan radical and radical cation models by means of gradient-corrected DFT (PWP86) and large basis sets (IGLO-III). Taken together, the calculations support previous experimental assignments of a charged tryptophan radical in DNA photolyase[7−10] and in cytochrome *c* peroxidase,[1−4] but a neutral radical in mutant Y122F *E. coli* RNR.[5,6] Several uncertainties do remain, however, and it is essentially only for the low-temperature W111 radical in mutant RNR that there is a perfect match between experiment and theory throughout.

The computed spin densities agree well with previous theoretical data obtained at similar levels.[6,15−18] The agreement with experiment is increased when using a more complete model (i.e., 3-ethylindole) vs the smaller systems. No previous theoretical data has been reported for the 3-ethylindole radical and radical cation. Similarly, the calculations show the need to use an appropriately large model for accurate comparisons with hyperfine data. We have reported full hyperfine tensors evaluated from first principles on tryptophan model systems, which enable a direct comparison with experimental data. When there is sufficiently detailed and unambiguous experimental data, the agreement with theory is most satisfactory. For some biological samples (DNA photolyase, and radical W_b in RNR), more detailed experiments are required for improved comparisons. We have in this work proposed several possible such experiments, such as deuteration of the β-protons in DNA photolyase Trp306, detailed study of the temperature dependence of Trp191 in CcP coupled with theoretical dynamics simulations of possible Trp-H^+−Asp equilibrium situation, and a more detailed scrutiny of the temperature dependence of the Trp111−Trp107 radical shift in Y122F mutant RNR.

The evaluated β-proton hyperfine tensors, Figures 1B and 2B, enabled a direct comparison with X-ray crystallography data,[11,37] confirming the CcP radical to be located at the global energy minimum with respect to rotation about the C3−Cβ bond (i.e. close to 90°). For the two RNR tryptophan radicals, the calculations confirm the possible identification of W_a as Trp111 (dihedral angle $\theta = 20°$) and W_b as Trp107 ($\theta = 115°$). Effects of hydrogen bonding were investigated for the Trp cation in CcP and the neutral W111 in RNR and were found to give an improved description.

Finally, the tryptophan−O_2 peroxide adduct was investigated. It was concluded that the C3 peroxide adduct loses all its radical character from the tryptophan unit to the oxygens and that the spin density distributions and hyperfine couplings are very similar to those of other alkyl (and related) peroxides. This agrees well with results from spin-trapping experiments, EPR observations, and mechanistic proposals for, e.g., the oxidation process in metmyoglobin.[14]

Acknowledgment. Financial support from the Swedish Natural Science Research Council (NFR) is gratefully acknowledged. We also thank Prof. A. Gräslund for valuable discussions.

References and Notes

(1) Hoffman, B. M.; Roberts, J. E.; Kang, C. H.; Margoliash, E. *J. Biol. Chem.* **1981**, *256*, 6556.
(2) Sivaraja, M.; Goodin, D. B.; Smith, M.; Hoffman, B. M. *Science* **1989**, *245*, 738.
(3) Houseman, A. L. P.; Doan, P. E.; Goodin, D. B.; Hoffman, B. M. *Biochemistry* **1993**, *32*, 4430.
(4) Huyett, J. E.; Doan, P. E.; Burbiel, R.; Houseman, A. L. P.; Sivaraja, M.; Goodin, D. B.; Hoffman, B. M. *J. Am. Chem. Soc.* **1995**, *117*, 9033.
(5) Sahlin, M.; Lassmann, G.; Pötsch, S.; Slaby, A.; Sjöberg, B.-M.; Gräslund, A. *J. Biol. Chem.* **1994**, *269*, 11699.
(6) Lendzian, F.; Sahlin, M.; MacMillan, F.; Bittl, R.; Fiege, R.; Pötsch, S.; Sjöberg, B.-M.; Gräslund, A.; Lubitz, W.; Lassmann, G. *J. Am. Chem. Soc.* **1996**, *118*, 8111.
(7) Heelis, P. F.; Okamura, T.; Sancar, A. *Biochemistry* **1990**, *29*, 5694.
(8) Li, Y. F.; Heelis, P. F.; Sancar, A. *Biochemistry* **1991**, *30*, 6322.
(9) Essenmacher, C.; Kim, S. T.; Atamian, M.; Babcock, G. T.; Sancar, A. *J. Am. Chem. Soc.* **1993**, *115*, 1602.
(10) Kim, S. T.; Sancar, A.; Essenmacher, C.; Babcock, G. T. *Proc. Natl. Acad. Sci. U.S.A.* **1993**, *90*, 8023.
(11) Nordlund, P.; Eklund, H.; *J. Mol. Biol.* **1993**, *232*, 123; Nordlund, P.; Sjöberg, B.-M.; Eklund, H. *Nature* **1990**, *345*, 593.
(12) Baron, A. J.; Stevens, C.; Wilmot, C.; Seneviratne, K. D.; Blakeley, V.; Dooley, D. M.; Phillips, S. E. V.; Knowles, P. F.; McPherson, M. J. *J. Biol. Chem.* **1994**, *269*, 25095.
(13) Warncke, K.; Brooks, H. B.; Lee, H.; McCracken, J.; Davidson, V. L.; Babcock, G. T. *J. Am. Chem. Soc.* **1995**, *117*, 10063.
(14) Gunther, M. R.; Kelman, D. J.; Corbett, J. T.; Mason, R. P. *J. Biol. Chem.* **1995**, *270*, 16075.
(15) Jensen, G. M.; Goodin, D. B.; Bunte, S. W. *J. Phys. Chem.* **1996**, *100*, 954.
(16) Walden, S. E.; Wheeler, R. A. *J. Phys. Chem.* **1996**, *100*, 1530.
(17) Walden, S. E.; Wheeler, R. A. *J. Chem. Soc., Perkin Trans. II* **1996**, (12), 2653; 2663.
(18) Krauss, M; Garmer, D. R. *J. Phys. Chem.* **1993**, *97*, 831.
(19) O'Malley, P. J.; Ellson, D. A. *Chem. Phys. Lett.* **1996**, *260*, 492.
(20) Serrano-Andrés, L.; Roos, B. O. *J. Am. Chem. Soc.* **1996**, *118*, 185.
(21) Himo, F.; Gräslund, A.; Eriksson, L. A. *Biophys. J.* **1997**, *72*, 1556.
(22) Malkin, V. G.; Malkina, O. L.; Eriksson, L. A.; Salahub, D. R. In *Theoretical and Computational Chemistry, Vol. 2; Modern Density*

Functional Theory: A Tool for Chemistry; Politzer, P., Seminario, J. M., Eds.; Elsevier: New York, 1995 and references therein.

(23) Eriksson, L. A.; Malkina, O. L.; Malkin, V. G.; Salahub, D. R. *J. Chem. Phys.* **1994**, *100*, 5066. Eriksson, L. A.; Wang, J.; Boyd, R. J. *Chem. Phys. Lett.* **1995**, *235*, 422. Eriksson, L. A. *J. Chem. Phys.* **1995**, *103*, 1050.

(24) Eriksson, L. A. In *Density Functional Methods: Applications in Chemistry and Materials Science*; Springborg, M., Ed.; John Wiley and Sons: New York, 1997 and references therein.

(25) Barone, V. *J. Chem. Phys.* **1994**, *101*, 6834.

(26) Barone, V. In *Recent Advances in Computational Chemistry*; Chong, D. P., Ed.; World Scientific: Singapore, 1996; Vol. 1, Part 1.

(27) Eriksson, L. A.; Malkin, V. G.; Malkina, O. L.; Salahub, D. R. *Int J. Quantum Chem.* **1994**, *52*, 879.

(28) St-Amant, A.; Salahub, D. R. *Chem. Phys. Lett.* **1990**, *169*, 387. St-Amant, A. Ph.D. Thesis, Universitéde Montréal, 1991. Salahub, D. R.; Fournier, R.; Mlynarski, P.; Papai, I.; St-Amant, A.; Ushio, J. In *Density Functional Methods in Chemistry*; Labanowski, J., Andzelm, J., Eds.; Springer: New York, 1991. Daul, C.; Goursot, A.; Salahub, D. R. In *Numerical Grid Methods and Their Application to Schrödinger's Equation*; Cerjan, C., Ed.; Nato ASI C142, 1993.

(29) Perdew, J. P. *Phys. Rev.* **1986**, *B33*, 8822; *Ibid*. **1986**, *B34*, 7406.

(30) Perdew, J. P.; Wang, Y. *Phys. Rev.* **1986**, *B33*, 8800.

(31) Kutzelnigg, W.; Fleischer, U.; Schindler, M. In *NMR−Basic Principles and Progress*; Springer-Verlag: Heidelberg, 1990; Vol. 23.

(32) Huzinaga, S. *J. Chem. Phys.* **1965**, *42*, 1293. Huzinaga, S.; Sakai, Y. *J. Chem. Phys.* **1969**, *50*, 1371.

(33) Godbout, N.; Salahub, D. R.; Andzelm, J.; Wimmer, E. *Can. J. Chem.* **1992**, *70*, 560.

(34) Broyden, C. G. *J. Inst. Math. Appl.* **1970**, *6*, 76, 222. Fletcher, R. *Comput. J.* **1970**, *13*, 317. Goldfarb, D. *Math. Comput.* **1970**, *24*, 23. Shanno, D. F. *Math. Comput.* **1970**, *24*, 647.

(35) Eriksson, L. A. *Mol. Phys.* **1997**, *91*, 827.

(36) Qin, Y.; Wheeler, R. A. *J. Chem. Phys.* **1995**, *102*, 1689. Qin, Y.; Wheeler, R. A. *J. Phys. Chem.* **1996**, *100*, 10554.

(37) Finzel, B. C.; Puolos, T. L.; Kraut, J. *J. Biol. Chem.* **1984**, *259*, 13027. Wang, J.; Mauro, J. M.; Edwards, S. L.; Oatley, S. J.; Fischel, L. A.; Ashford, V. A.; Xuong, N. H.; Kraut, J. *Biochemistry* **1990**, *29*, 7160.

(38) Ho, P. S.; Hoffman, B. M.; Kang, C. H.; Margoliash, E *J. Biol. Chem.* **1983**, *258*, 4356.

(39) Sevilla, M. D.; Becker, D.; Yan, M. *J. Chem. Soc., Faraday Trans.* **1990**, *86*, 3279.

(40) Wetmore, S. D.; Boyd, R. J.; Eriksson, L. A. *J. Chem. Phys.* **1997**, *106*, 7738.

(41) Howard, J. A. *Can. J. Chem.* **1979**, *57*, 253.